Physics Letters B 797 (2019) 134849

Contents lists available at ScienceDirect

Physics Letters B

www.elsevier.com/locate/physletb

Probing the seesaw mechanism at the 250 GeV ILC

Arindam Das [a,*], Nobuchika Okada [b], Satomi Okada [b], Digesh Raut [c]

[a] Department of Physics, Osaka University, Toyonaka, Osaka 560-0043, Japan
[b] Department of Physics and Astronomy, University of Alabama, Tuscaloosa, AL 35487, USA
[c] Bartol Research Institute, Department of Physics and Astronomy, University of Delaware, Newark, DE 19716, USA

ARTICLE INFO

Article history:
Received 13 April 2019
Received in revised form 12 June 2019
Accepted 7 August 2019
Available online 16 August 2019
Editor: G.F. Giudice

ABSTRACT

We consider a gauged $U(1)_{B-L}$ (Baryon-minus-Lepton number) extension of the Standard Model (SM), which is anomaly-free in the presence of three Right-Handed Neutrinos (RHNs). Associated with the $U(1)_{B-L}$ symmetry breaking the RHNs acquire their Majorana masses and then play the crucial role to generate the neutrino mass matrix by the seesaw mechanism. Towards the experimental confirmation of the seesaw mechanism, we investigate a RHN pair production through the $U(1)_{B-L}$ gauge boson (Z') at the 250 GeV International Linear Collider (ILC). The Z' gauge boson has been searched at the Large Hadron Collider (LHC) Run-2 and its production cross section is already severely constrained. The constraint will become more stringent by the future experiments with the High-Luminosity upgrade of the LHC (HL-LHC). We find a possibility that even after a null Z' boson search result at the HL-LHC, the 250 GeV ILC can search for the RHN pair production through the final state with same-sign dileptons plus jets, which is a "smoking-gun" signature from the Majorana nature of RHNs. In addition, some of RHNs are long-lived and leave a clean signature with a displaced vertex. Therefore, the 250 GeV ILC can operate as not only a Higgs Factory but also a RHN discovery machine to explore the origin of the Majorana neutrino mass generation, namely the seesaw mechanism.

Type-I seesaw [1] is probably the simplest mechanism to naturally generate tiny masses for the neutrinos in the Standard Model (SM), where Right-Handed Neutrinos (RHNs) with large Majorana masses play the crucial role. It has been known for a long time that the RHNs are naturally incorporated into the so-called minimal $B-L$ model [2], in which the global $U(1)_{B-L}$ (Baryon-minus-Lepton number) symmetry in the SM is gauged. In addition to the SM particle content, the model contains a minimal new particle content, namely, the $U(1)_{B-L}$ gauge boson (Z' boson), three RHNs, and a $U(1)_{B-L}$ Higgs field. The existence of the three RHNs is crucial for the model to be free from all the gauge and the mixed gauge-gravitational anomalies. Associated with the $U(1)_{B-L}$ symmetry breaking triggered by the vacuum expectation value (VEV) of the $B-L$ Higgs field, the Z' boson mass and the Majorana masses for the RHNs are generated. Once the electroweak symmetry is broken, the type-I seesaw mechanism generates the mass matrix for the light SM neutrinos.

If the seesaw scale, in other words, the mass scale of the Majorana RHNs lies at the TeV scale or lower, RHNs (more precisely, heavy Majorana neutrino mass eigenstates after the seesaw mechanism) can be produced at high energy colliders through the process mediated by the Z' boson. Once produced, the RHN decays into the SM particles through the SM weak gauge boson or the SM Higgs boson mediated processes. Since the RHNs are originally singlet under the SM gauge group, the decay process implies a mass mixing between the RHNs and the SM neutrinos through the type-I seesaw mechanism. Among possible final states from the RHN decay, it is of particular interest to consider the same-sign dilepton final state, a "smoking-gun" signature for the RHNs Majorana nature, for which the SM backgrounds are few. For prospects of discovering the Majorana RHN at the future Large Hadron Collider (LHC) experiments, see, for example, Refs. [3–8].

In this paper, we investigate the RHN production at future e^+e^- colliders, in particular, the International Linear Collider (ILC), in the context of a gauged $B-L$ extension of the SM. The ILC is proposed with a staged machine design, with the first stage at 250 GeV with a luminosity goal of 2000/fb [9]. Setting the ILC energy at 250 GeV maximizes the SM Higgs boson production cross section, and hence the 250 GeV ILC will be operating as a Higgs Factory. x This machine allows us to precisely measure the Higgs boson properties to test the SM Higgs sector. One may think that the 250 GeV ILC is not a powerful machine compared to the LHC in exploring

* Corresponding author.
E-mail address: dasarindamphysics@gmail.com (A. Das).

https://doi.org/10.1016/j.physletb.2019.134849

Table 1
The particle content of the minimal $B-L$ model. In addition to the three generations of SM particles ($i=1,2,3$), three RHNs (N_R^i) and one $B-L$ Higgs field (Φ) are introduced.

	$SU(3)_C$	$SU(2)_L$	$U(1)_Y$	$U(1)_{B-L}$
q_L^i	**3**	**2**	1/6	1/3
u_R^i	**3**	**1**	2/3	1/3
d_R^i	**3**	**1**	−1/3	1/3
ℓ_L^i	**1**	**2**	−1/2	−1
e_R^i	**1**	**1**	−1	−1
H	**1**	**2**	−1/2	0
N_R^i	**1**	**1**	0	−1
Φ	**1**	**1**	0	+2

Table 2
New particle content of the alternative $B-L$ model. The three RHNs and the $B-L$ Higgs field in Table 1 are replaced by three RHNs ($N_R^{1,2,3}$) with flavor-dependent charges and three Higgs fields ($H_\nu, \Phi_{A,B}$).

	$SU(3)_C$	$SU(2)_L$	$U(1)_Y$	$U(1)_{B-L}$
$N_R^{1,2}$	**1**	**1**	0	−4
N_R^3	**1**	**1**	0	+5
H_ν	**1**	**2**	$-\frac{1}{2}$	3
Φ_A	**1**	**1**	0	+8
Φ_B	**1**	**1**	0	−10

new physics if it is less related to the SM Higgs sector. Given the present status with no evidence of new physics in the LHC data and the prospect of new physics search at the High-Luminosity LHC (HL-LHC) in the near future, it seems quite non-trivial to consider new physics for which the 250 GeV ILC is more capable than the HL-LHC. The main point of this paper is to show that the 250 GeV ILC can, in fact, probe the RHN pair production mediated by the Z' boson even in the worst case scenario that the HL-LHC data with a goal 3000/fb luminosity would show no evidence for a resonant Z' boson production.

In this paper, we consider two simple gauged $B-L$ extended SMs. One is the minimal $B-L$ model whose particle content is listed in Table 1. The model is free from all the gauge and the mixed gauge-gravitational anomalies, thanks to the presence of the three RHNs.

In addition to the SM, we introduce Yukawa couplings involving new fields:

$$\mathcal{L}_Y = -\sum_{i,j=1}^{3} Y_D^{ij}\overline{\ell_L^i} H N_R^j - \frac{1}{2}\sum_{k=1}^{3} Y_N^k \Phi \overline{N_R^{k\,c}} N_R^k + \text{h.c.}, \tag{1}$$

where three RHNs (N_R^j) have the Dirac Yukawa couplings with the SM lepton doublets as well as the Majorana Yukawa couplings with the $B-L$ Higgs field. We assume a suitable Higgs potential to yield VEVs for the Higgs fields, $\langle H\rangle = (v/\sqrt{2},0)^T$ with $v=246$ GeV and $\langle\Phi\rangle = v_\phi/\sqrt{2}$, to break the electroweak and the $U(1)_{B-L}$ symmetries, respectively. The symmetry breakings generate the Z' boson mass, the Majorana masses for RHNs, and the neutrino Dirac masses:

$$m_{Z'} = 2\,g_{BL}\,v_\phi,\;\; m_{N^j} = \frac{Y_N^j}{\sqrt{2}}v_\phi,\;\; m_D^{ij} = \frac{Y_D^{ij}}{\sqrt{2}}v, \tag{2}$$

where g_{BL} is the $B-L$ gauge coupling.

The other model is what we call "alternative $B-L$ model", in which a $U(1)_{B-L}$ charge -4 is assigned to two RHNs ($N_R^{1,2}$), while a $U(1)_{B-L}$ charge -5 is assigned for the third RHN (N_R^3) [10]. The cancellation of all the gauge and the mixed gauge-gravitational anomalies is achieved also by this charge assignment. In the alternative $B-L$ model, we introduce a minimal Higgs sector with one new Higgs doublet H_ν and two $U(1)_{B-L}$ Higgs fields $\Phi_{A,B}$. Table 2 lists the new particle content.

In the alternative $B-L$ model, we introduce the following Yukawa couplings involving new fields:

$$\mathcal{L}_Y = -\sum_{i=1}^{3}\sum_{j=1}^{2} Y_D^{ij}\overline{\ell_L^i} H_\nu N_R^j - \frac{1}{2}\sum_{k=1}^{2} Y_N^k \Phi_A \overline{N_R^{k\,c}} N_R^k - \frac{1}{2} Y_N^3 \Phi_B \overline{N_R^{3\,c}} N_R^3 + \text{h.c.} \tag{3}$$

We assume a suitable Higgs potential to trigger the gauge symmetry breaking with non-zero VEVs as $\langle H\rangle = (v_h/\sqrt{2},0)^T$, $\langle H_\nu\rangle = (v_\nu/\sqrt{2},0)^T$, and $\langle\Phi_{A,B}\rangle = v_{A,B}/\sqrt{2}$, where we require $\sqrt{v_h^2+v_\nu^2} = 246$ GeV for the electroweak symmetry breaking. After the $U(1)_{B-L}$ and SM gauge symmetries are spontaneously broken, the Z' boson mass, the Majorana masses for the RHNs, and the Dirac neutrino masses are generated:

$$m_{Z'} = g_{BL}\sqrt{64v_A^2+100v_B^2+9v_\nu^2} \simeq g_{BL}\sqrt{64v_A^2+100v_B^2},$$
$$m_{N^{1,2}} = \frac{Y_N^{1,2}}{\sqrt{2}}v_A,\;\; m_{N^3} = \frac{Y_N^3}{\sqrt{2}}v_B,\;\; m_D^{ij} = \frac{Y_D^{ij}}{\sqrt{2}}v_\nu. \tag{4}$$

Here, we have used the LEP constraint: $v_A^2+v_B^2 \gg (246\,\text{GeV})^2$ [11]. Note that only the two RHNs are involved in the seesaw mechanism (the so-called "minimal seesaw" [12]), while the third RHN (N_R^3) has no direct coupling with the SM fields and hence it is naturally a dark matter (DM) candidate. Recently, this RHN DM scenario has been proposed in Ref. [13].

Before going to our analysis for the 250 GeV ILC, we first need to understand the current status and the future prospect of the $B-L$ models in terms of the LHC experiments. The ATLAS and the CMS collaborations have been searching for a Z' boson resonance with a variety of final states at the LHC Run-2 with $\sqrt{s}=13$ TeV and the most severe upper bound relevant to our Z' boson production cross section has been obtained from the resonance search with a dilepton (e^+e^- or $\mu^+\mu^-$) final state. The latest results by the ATLAS collaboration [14] and the CMS collaboration [15] with a 36/fb integrated luminosity are consistent with each other and set the lower mass bound of around 4.5 TeV for the sequential SM Z' boson. For our analysis, we employ the ATLAS result [14].

In the $B-L$ models, the differential cross section for the process, $pp \to Z' + X \to \ell^+\ell^- + X$, where $\ell^+\ell^- = e^+e^-$ or $\mu^+\mu^-$, with respect to the dilepton invariant mass $M_{\ell\ell}$ is given by

$$\frac{d\sigma}{dM_{\ell\ell}} = \sum_{q,\bar{q}} \int_{\frac{M_{\ell\ell}^2}{E_{\text{LHC}}^2}}^{1} dx\, \frac{2M_{\ell\ell}}{xE_{\text{LHC}}^2} f_q(x,Q^2)\, f_{\bar{q}}\left(\frac{M_{\ell\ell}^2}{xE_{\text{LHC}}^2}, Q^2\right) \times \hat{\sigma}(q\bar{q}\to Z'\to\ell^+\ell^-), \tag{5}$$

where Q is the factorization scale (we fix $Q=m_{Z'}$, for simplicity), $E_{\text{LHC}}=13$ TeV is the LHC Run-2 energy, f_q ($f_{\bar{q}}$) is the parton distribution function for quark (anti-quark), and the cross section for the colliding partons is given by

$$\hat{\sigma}(q\bar{q}\to Z'\to\ell^+\ell^-) = \frac{g_{BL}^4}{324\pi}\frac{M_{\ell\ell}^2}{(M_{\ell\ell}^2-m_{Z'}^2)^2+m_{Z'}^2\Gamma_{Z'}^2}. \tag{6}$$

Here, the total decay width of the Z' boson ($\Gamma_{Z'}$) is given by

$$\Gamma_{Z'} = \frac{g_{BL}^2}{24\pi} m_{Z'}\left[13 + \sum_{j=1}^{3} Q_{N^j}^2\left(1-\frac{4m_{N^j}^2}{m_{Z'}^2}\right)^{\frac{3}{2}}\right], \tag{7}$$

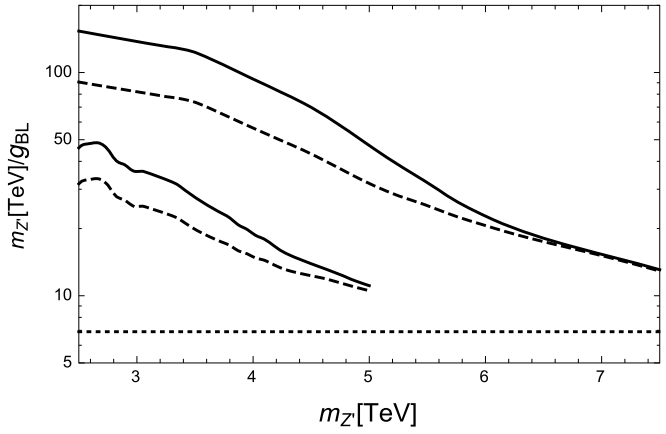

Fig. 1. The lower bounds on $m_{Z'}/g_{BL}$ as a function of $m_{Z'}$ from the ATLAS 2017 result and the HL-LHC search reach [19], along with the LEP constraint of $m_{Z'}/g_{BL} > 6.9$ TeV (dotted horizontal line) [11].

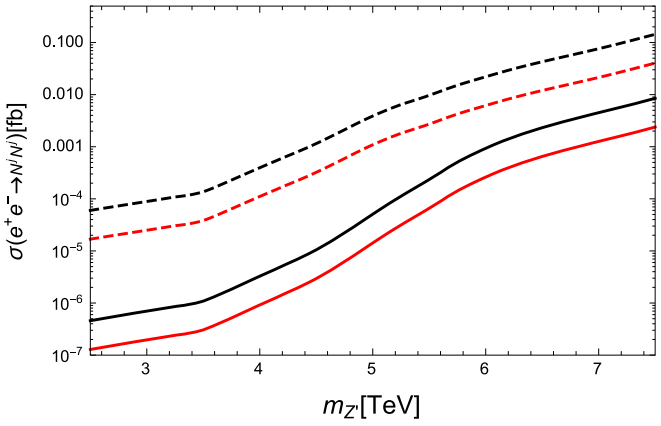

Fig. 2. The RHN pair production cross sections at the 250 GeV ILC, along the prospective HL-LHC bounds shown in Fig. 1. The upper (black) and lower (red) solid lines are the results for the minimal $B-L$ model with $m_{N^{1,2,3}} = 50$ GeV and 100 GeV, respectively. The results for the alternative $B-L$ model are shown as the upper (black) and lower (red) dashed lines corresponding to $m_{N^{1,2}} = 50$ GeV and 100 GeV, respectively.

where we have neglected all SM fermion masses, and Q_{N^j} is the $U(1)_{B-L}$ charge of the RHN N_R^j. For the minimal (alternative) $B-L$ model, let us consider two benchmark (degenerate) mass spectra for the RHNs: $m_{N^{1,2,3}}(m_{N^{1,2}}) = m_N = 50$ GeV and 100 GeV. It has been recently shown in Ref. [13] that in the alternative $B-L$ model, N_R^3 plays the role of DM in the Universe, reproducing the observed DM relic abundance with $m_{N^3} \simeq m_{Z'}/2$. Motivated by the discussion, we set $m_{N^3} \simeq m_{Z'}/2$, so that the N^3 contribution to $\Gamma_{Z'}$ is neglected.

In our LHC analysis, we employ CTEQ6L [16] for the parton distribution functions and calculate the cross section of the dilepton production through the Z' boson exchange in the s-channel. Neglecting the mass for the RHNs in our LHC analysis, the resultant cross section is controlled by only two parameters: g_{BL} and $m_{Z'}$. To derive a constraint for these parameters from the ATLAS 2017 results [14], we follow the strategy in Refs. [17,18]: we first calculate the cross section of the process, $pp \to Z' + X \to \ell^+\ell^- + X$, for the sequential SM Z' boson and find a k-factor ($k = 1.31$) by which our cross section coincides with the cross section for the sequential SM Z' boson presented in the ATLAS paper [14]. We employ this k-factor for all of our LHC analysis, and find an upper bound on g_{BL} as a function of $m_{Z'}$ from the ATLAS 2017 results. For the prospect of the future constraints to be obtained after the HL-LHC experiment with the 3000/fb integrated luminosity, we refer the simulation result presented in the ATLAS Technical Design Report [19]. Figure 4.20 (b) in this report shows the prospective upper bound on the cross section, $pp \to Z' + X \to e^+e^- + X$, as low as 10^{-5} fb over the range of $2.5 \le m_{Z'}$ [TeV] ≤ 7.5, which results in a lower bound on $m_{Z'} > 6.4$ TeV for the sequential SM Z' boson.

For the following ILC analysis, instead of the LHC upper bound on g_{BL} as a function of $m_{Z'}$, it is more useful to plot the LHC lower bound on $m_{Z'}/g_{BL}$, which is shown in Fig. 1. The lower and upper solid lines correspond to the lower bound from the ATLAS 2017 and the prospective HL-LHC bound, respectively, for the minimal $B-L$ model. The corresponding lower bounds for the alternative $B-L$ model are depicted as the dashed lines. In the alternative $B-L$ model, the Z' boson decay to a pair of RHNs dominates the total decay width and hence the branching ratio into dileptons is relatively suppressed, resulting in the LHC constraints weaker than those for the minimal $B-L$ model. Note that the LHC constraint for $m_{Z'}/g_{BL}$ becomes dramatically weaker as $m_{Z'}$ increases. Since the ILC energy is much smaller than $m_{Z'}$, the Z' boson mediated processes at the ILC are described by effective higher dimensional operators which are proportional to $(m_{Z'}/g_{BL})^2$. Therefore, the plots in Fig. 1 imply that the ILC can be a more powerful machine than the LHC to explore the $B-L$ models, if the Z' boson mass is beyond the search reach of the HL-LHC experiment.

Let us now investigate the RHN pair production at the 250 GeV ILC. The relevant process is $e^+e^- \to Z'^* \to N^iN^i$ mediated by a virtual Z' boson in the s-channel. Since the collider energy $\sqrt{s} = 250$ GeV is much smaller than $m_{Z'}$, the RHN pair production cross section is approximately given by

$$\sigma(e^+e^- \to Z'^* \to N^iN^i) \simeq \frac{(Q_{N^i})^2}{24\pi} s \left(\frac{g_{BL}}{m_{Z'}}\right)^4 \left(1 - \frac{4m_{N^i}^2}{m_{Z'}^2}\right)^{\frac{3}{2}}. \quad (8)$$

For our benchmark RHN mass spectra, we show in Fig. 2 the RHN pair production cross sections at the 250 GeV ILC, along the prospective HL-LHC bounds on $m_{Z'}/g_{BL}$ shown in Fig. 1. For $m_{Z'} = 7.5$ TeV, we have found $\sigma(e^+e^- \to Z'^* \to N^iN^i) = 0.0085$ and 0.14 fb for $m_{N^{1,2,3}} = 50$ GeV and $m_{N^{1,2}} = 50$ GeV, respectively, for the minimal and alternative $B-L$ models. For the degenerate RHN mass spectra, we have $\sum_{i=1}^{3} \sigma(e^+e^- \to Z'^* \to N^iN^i) = 0.026$ fb and $\sum_{i=1}^{2} \sigma(e^+e^- \to Z'^* \to N^iN^i) = 0.29$ fb for each model, and thus 52 and 576 events with the 2000/fb goal luminosity of the 250 GeV ILC, while satisfying the prospective constraints after the HL-LHC with the 3000/fb integrated luminosity. Considering the smoking-gun signature of the RHN pair production for which the SM backgrounds are few, the 250 GeV ILC can operate as a Majorana RHN discovery machine towards confirming the type-I seesaw mechanism. In the second stage of the ILC with $\sqrt{s} = 500$ GeV [9] we expect roughly 4 times more events with the same goal luminosity.

For detailed discussion about the ILC phenomenology, we need to consider the decay processes of the heavy neutrinos. Assuming $|m_D^{ij}/m_{N^j}| \ll 1$ in Eq. (2) or Eq. (4), the type-I seesaw mechanism leads to the light Majorana neutrino mass matrix of the form:

$$m_\nu \simeq m_D M_N^{-1} m_D^T = \frac{1}{m_N} m_D\, m_D^T, \quad (9)$$

where $M_N = m_N \mathbf{1}$ with the 3×3 (2×2) identity matrix $\mathbf{1}$ for the minimal (alternative) $B-L$ model. Through the seesaw mechanism, the SM neutrinos and the RHNs are mixed in the mass eigenstates. The flavor eigenstates of the SM neutrinos (ν) are expressed in terms of the light (ν_m) and heavy (N_m) Majorana neu-

Table 3
Branching ratios of the decay of the heavy neutrinos $N^{i=1,2,3}$ into $e/\mu/\tau + jj$ in the minimal $B-L$ model. The resultant branching ratios are independent of the pattern of the light neutrino spectra and $m_{\rm lightest}$.

	$e+jj$	$\mu+jj$	$\tau+jj$
$m_N = 50$ GeV			
N^1	0.412	0.104	0.104
N^2	0.204	0.224	0.224
N^3	0.015	0.310	0.310
$m_N = 100$ GeV			
N^1	0.402	0.102	0.102
N^2	0.189	0.208	0.208
N^3	0.0143	0.296	0.296

trino mass eigenstates as $\nu \simeq \mathcal{R} N_m + \mathcal{N}\nu_m$, where $\mathcal{R} = m_D (M_N)^{-1}$, $\mathcal{N} = \left(1 - \frac{1}{2}\mathcal{R}^*\mathcal{R}^T\right) U_{\rm MNS} \simeq U_{\rm MNS}$, and $U_{\rm MNS}$ is the neutrino mixing matrix which diagonalizes the light neutrino mass matrix as

$$U_{\rm MNS}^T m_\nu U_{\rm MNS} = {\rm diag}(m_1, m_2, m_3). \tag{10}$$

Through the mixing matrix $\mathcal{R}$ and the original Dirac Yukawa interactions, the heavy neutrino mass eigenstates, if kinematically allowed, decay into ℓW, νZ, νh (h is the SM Higgs boson). If the decays to on-shell $W/Z/h$ are not allowed, the heavy neutrinos decay into SM fermions mainly through off-shell W/Z. In Appendices A–C, we list the heavy neutrino decay width formulas for two cases: (A) the heavy neutrinos decay into three SM fermions through off-shell W/Z, and (B) the heavy neutrinos decay into ℓW, νZ, νh. As shown in Appendix D, in our simple parametrization of m_D from the type-I seesaw formula, $|\mathcal{R}_{\alpha i}|^2$ is expressed as a function of only the lightest light neutrino mass eigenvalue $m_{\rm lightest}$ and m_N by using the neutrino oscillation data. Therefore, once we fix $m_{\rm lightest}$ and m_N, the heavy neutrino decay processes are completely determined.

We now consider the smoking-gun signature of the heavy neutrino pair production, namely, $e^+e^- \to Z'^* \to N^i N^i$, followed by $N^i N^i \to \ell^\pm \ell^\pm W^{\mp(*)} W^{\mp(*)} \to \ell^\pm \ell^\pm jjjj$. This lepton number violating process originates from the Majorana nature of the heavy neutrinos and is basically free from the SM background. The final same-sign dileptons can also violate the lepton flavor because of the neutrino mixing matrix. Using the formulas given in Appendices B–D, we calculate the branching ratios of the process, $N^i \to e/\mu/\tau + jj$. For the minimal $B-L$ model, the resultant branching ratios into $N^i \to \ell W^{(*)} \to \ell jj$ for each flavor charged lepton are listed in Table 3, for $m_N = 50$ GeV and 100 GeV. For the degenerate RHN masses, we find that the resultant branching ratios are independent of the pattern of the light neutrino mass spectra and $m_{\rm lightest}$. We find the branching ratio of $N^i N^i \to \ell^\pm \ell^\pm jjjj$ for any lepton flavors to be about 20%. For the alternative $B-L$ model, we obtain a similar result. See Appendix E for details.

Finally, let us discuss another interesting signature of the heavy neutrino production. Eq. (9) indicates elements of $\mathcal{R}$ is very small, so that heavy neutrinos can be long-lived. Such long-lived heavy neutrinos leave displaced vertex signatures which can be easily distinguished from the SM background events. For the minimal $B-L$ model, we show the decay lengths (lifetime times speed of light) of heavy neutrinos in Appendix F (see Figs. 3 and 4). Interestingly, the longest-lived heavy neutrino lifetime is inversely proportional to $m_{\rm lightest}$ [8], so that $m_{\rm lightest}$ can be determined once the long-lived heavy neutrino is observed with a displaced vertex. Note that this heavy neutrino becomes stable and thus a DM candidate in the limit of $m_{\rm lightest} \to 0$. We can see that in this limit, a Z_2 symmetry comes out as an enhanced symmetry, under which the DM particle is odd. Thus, the stability of the DM particle is ensured by this Z_2 symmetry, as previously discussed in Ref. [20].

In conclusion, we have considered the minimal and the alternative $B-L$ models which are simple and well-motivated extension of the SM to incorporate the SM neutrino masses and flavor mixings through the type-I seesaw mechanism. Towards the experimental confirmation of the seesaw mechanism, we have investigated the heavy neutrino pair production mediated by the Z' boson at the 250 GeV ILC. The Z' boson mediated process is very severely constrained by the LHC Run-2 results and the constraints will be more stringent in the future. Nevertheless, we have found that if Z' boson is very heavy, for example, $m_{Z'} \gtrsim 7.5$ TeV, the heavy neutrino pair production cross section at the 250 ILC can be sizable, while satisfying the prospective bounds after the HL-LHC experiment with the 3000/fb integrated luminosity. Once a pair of heavy neutrinos is produced, the same-sign dilepton final states can be observed, which are the signature of the Majorana nature of the heavy neutrinos. In addition, the heavy neutrinos can be long-lived and leave displaced vertex signatures. Therefore, it is possible that the 250 GeV ILC operates as not only a Higgs Factory but also a heavy neutrino discovery machine to explore the origin of the Majorana neutrino mass generation, namely the seesaw mechanism.

The Z' boson can be indirectly searched with the dilepton final states, $e^+e^- \to \ell^+\ell^-$, at the 250 GeV ILC by observing a deviation of the total cross section from its SM prediction. For $m_{Z'} = 7.5$ TeV, we have obtained a deviation of $\mathcal{O}(1\%)$ from the SM prediction through an interference between the SM process and the Z' boson mediated process. This deviation can be explored at the ILC [9].

Acknowledgements

This work is supported in part by the Japan Society for the Promotion of Science Postdoctoral Fellowship for Research in Japan (A.D.), the United States Department of Energy Grant (DE-SC0013680 (N.O.) and DE-SC0013880 (D.R.)), and the M. Hildred Blewett Fellowship of the American Physical Society, https://www.aps.org (S.O.).

Appendix A. Weak interactions of the neutrino mass eigenstates

In terms of the neutrino mass eigenstates, the charged current (CC) interaction can be written as

$$\mathcal{L}_{\rm CC} = -\frac{g}{\sqrt{2}} W_\mu \overline{\ell_\alpha} \gamma^\mu P_L \left(\mathcal{N}_{\alpha j} \nu_{m_j} + \mathcal{R}_{\alpha j} N_{m_j}\right) + {\rm h.c.}, \tag{11}$$

where ℓ_α ($\alpha = e, \mu, \tau$) denotes the three generations of the charged leptons, and $P_L = \frac{1}{2}(1-\gamma_5)$ is the left-handed projection operator. Similarly, the neutral current (NC) interaction is given by

$$\begin{aligned}\mathcal{L}_{\rm NC} = -\frac{g}{2\cos\theta_{\rm W}} Z_\mu \Big[& \overline{\nu_{m_i}} \gamma^\mu P_L (\mathcal{N}^\dagger \mathcal{N})_{ij} \nu_{m_j} \\ & + \overline{N_{m_i}} \gamma^\mu P_L (\mathcal{R}^\dagger \mathcal{R})_{ij} N_{m_j} \\ & + \left\{ \overline{\nu_{m_i}} \gamma^\mu P_L (\mathcal{N}^\dagger \mathcal{R})_{ij} N_{m_j} + {\rm h.c.} \right\} \Big],\end{aligned} \tag{12}$$

where $\theta_{\rm W}$ is the weak mixing angle.

Appendix B. Heavy neutrino decay to three SM fermions

The heavy neutrinos are lighter than the weak bosons, they decay into three SM fermions via off-shell W and Z bosons mediated processes. The partial decay widths into three lepton final states are as follows:

$$\Gamma^{(W^*)}(N^i \to \ell_L^\alpha \ell_L^\beta \nu^\kappa) = |R_{\alpha i}|^2 \, |U_{\rm MNS}^{\beta\kappa}|^2 \, \Gamma_{\rm N^i},$$

$$\Gamma^{(Z^*)}(N^i \to \nu^\alpha \ell_L^\beta \ell_L^\kappa) = |\mathcal{R}_{\alpha i}|^2\, \delta_{\beta\kappa} \cos^2 2\theta_W\, \frac{1}{4}\, \Gamma_{N^i},$$
$$\Gamma^{(Z^*)}(N^i \to \nu^\alpha \ell_R^\beta \ell_R^\kappa) = |\mathcal{R}_{\alpha i}|^2 \delta_{\beta\kappa} \sin^4\theta_W\, \Gamma_{N^i},$$
$$\Gamma^{(Z^*)}(N^i \to \nu^\alpha \nu^\beta \nu^\kappa) = |\mathcal{R}_{\alpha i}|^2\, \delta_{\beta\kappa}\, \frac{1}{4}\, \Gamma_{N^i}, \tag{13}$$

where

$$\Gamma_{N^i} = \frac{G_F^2}{192\pi^3} m_{N^i}^5 \tag{14}$$

with the Fermi constant G_F, and $U_{\rm MNS}^{\beta\kappa}$ is a (β,κ)-element of the neutrino mixing matrix. In deriving the above formulas, we have neglected all lepton masses. For the lepton final states, we have an interference between the Z and W boson mediated decay processes:

$$\Gamma^{(Z^*/W^*)}(N^i \to \nu^\alpha \ell^\alpha \ell^\alpha) = |\mathcal{R}_{\alpha i}|^2\, 2{\rm Re}[U_{\rm MNS}^{ii}]\, \Gamma_{N^i}. \tag{15}$$

The partial decay widths into one lepton plus two quarks are as follows:

$$\Gamma^{(W^*)}(N^i \to \ell^\alpha q_L^\beta \bar{q}_L^\kappa) = N_c \times |\mathcal{R}_{\alpha i}|^2\, |V_{\rm CKM}^{\beta\kappa}|^2\, \Gamma_{N^i},$$
$$\Gamma^{(Z^*)}(N^i \to \nu^\alpha q_L^\beta \bar{q}_L^\kappa) = N_c \times |\mathcal{R}_{\alpha i}|^2\, \delta_{\beta\kappa}\, Q_L^2\, \Gamma_{N^i},$$
$$\Gamma^{(Z^*)}(N^i \to \nu^\alpha q_R^\beta \bar{q}_R^\kappa) = N_c \times |\mathcal{R}_{\alpha i}|^2\, \delta_{\beta\kappa}\, Q_R^2\, \Gamma_{N^i}, \tag{16}$$

where $N_c = 3$ is the color factor, $V_{\rm CKM}^{\beta\kappa}$ is a (β,κ)-element of the quark mixing matrix, $Q_L = 1/2 - (2/3)\sin^2\theta_W$ and $Q_R = -(2/3)\sin^2\theta_W$ for a up-type quark, and $Q_L = -1/2 - (1/3)\sin^2\theta_W$ and $Q_R = -(1/3)\sin^2\theta_W$ for a down-type quark.

Appendix C. Heavy neutrino decay to on-shell $W/Z/h$

If the heavy neutrinos are heavy enough to decay into ℓW, $\nu_\ell Z$, and $\nu_\ell h$, the partial decay widths are as follows:

$$\Gamma(N_m^i \to \ell_\alpha W) = \frac{1}{16\pi} \frac{(M_N^2 - m_W^2)^2 (M_N^2 + 2m_W^2)}{M_N^3 v_h^2} |\mathcal{R}_{\alpha i}|^2,$$
$$\Gamma(N_m^i \to \nu_{\ell_\alpha} Z) = \frac{1}{32\pi} \frac{(M_N^2 - m_Z^2)^2 (M_N^2 + 2m_Z^2)}{M_N^3 v_h^2} |\mathcal{R}_{\alpha i}|^2,$$
$$\Gamma(N_m^i \to \nu_{\ell_\alpha} h) = \frac{1}{32\pi} \frac{(M_N^2 - m_h^2)^2}{M_N v_h^2} |\mathcal{R}_{\alpha i}|^2. \tag{17}$$

Appendix D. Determining $R_{\alpha i}$ from the neutrino oscillation data

The elements of the matrix $\mathcal{R}$ are constrained so as to reproduce the neutrino oscillation data. In our analysis, we adopt the following values for the neutrino oscillation parameters: $\Delta m_{12}^2 = m_2^2 - m_1^2 = 7.6 \times 10^{-5}$ eV^2, $\Delta m_{23}^2 = |m_3^2 - m_2^2| = 2.4 \times 10^{-3}$ eV^2, $\sin^2 2\theta_{12} = 0.87$, $\sin^2 2\theta_{23} = 1.0$, and $\sin^2 2\theta_{13} = 0.092$ [21]. The neutrino mixing matrix is explicitly given by

$$U_{\rm MNS} = \begin{pmatrix} c_{12}c_{13} & c_{12}c_{13} & s_{13}e^{-i\delta} \\ -s_{12}c_{23} - c_{12}s_{23}s_{13}e^{i\delta} & c_{12}c_{23} - s_{12}s_{23}s_{13}e^{i\delta} & s_{23}c_{13} \\ s_{12}c_{23} - c_{12}c_{23}s_{13}e^{i\delta} & -c_{12}s_{23} - s_{12}c_{23}s_{13}e^{i\delta} & c_{23}c_{13} \end{pmatrix} \times \begin{pmatrix} 1 & 0 & 0 \\ 0 & e^{-i\rho_1} & 0 \\ 0 & 0 & e^{-i\rho_2} \end{pmatrix},$$

where $c_{ij} = \cos\theta_{ij}$, $s_{ij} = \sin\theta_{ij}$, and ρ_1 and ρ_2 are the Majorana phases ($\rho_2 = 0$ in the minimal seesaw). For simplicity, we set the Dirac CP-phase as $\delta = 3\pi/2$ from the indications by the recent T2K [22] and NOνA [23] data.

In our analysis we consider two patterns of the light neutrino mass spectrum, namely the Normal Hierarchy (NH) where the light neutrino mass eigenvalues are ordered as $m_1 < m_2 < m_3$ and the Inverted Hierarchy (IH) where the light neutrino mass eigenvalues are ordered as $m_3 < m_1 < m_2$. In the NH (IH) case, this lightest mass eigenvalue $m_{\rm lightest}$ is identified with m_1 (m_3). Thus, the mass eigenvalue matrix for the NH case is expressed as

$$D_{\rm NH} = {\rm diag}\left(m_{\rm lightest}, m_2^{\rm NH}, m_3^{\rm NH}\right), \tag{18}$$

with $m_2^{\rm NH} = \sqrt{\Delta m_{12}^2 + m_{\rm lightest}^2}$ and $m_3^{\rm NH} = \sqrt{\Delta m_{23}^2 + (m_2^{\rm NH})^2}$, while the mass eigenvalue matrix for the IH case is

$$D_{\rm IH} = {\rm diag}\left(m_1^{\rm IH}, m_2^{\rm IH}, m_{\rm lightest}\right) \tag{19}$$

with $m_2^{\rm IH} = \sqrt{\Delta m_{23}^2 + m_{\rm lightest}^2}$ and $m_1^{\rm IH} = \sqrt{(m_2^{\rm IH})^2 - \Delta m_{12}^2}$. Through the type-I seesaw mechanism, the light neutrino mass matrix is expressed as

$$m_\nu = m_D M_N^{-1} m_D^T = U_{\rm MNS}^* D_{\rm NH/IH} U_{\rm MNS}^\dagger, \tag{20}$$

for the NH/IH cases, respectively. This formula allows us to simply parametrize the mixing matrix $\mathcal{R}$ as

$$\mathcal{R}^{\rm NH/IH} = \frac{1}{\sqrt{m_N}}\, U_{\rm MNS}^*\, \sqrt{D_{\rm NH/IH}}, \tag{21}$$

where $\sqrt{D_{\rm NH}} = {\rm diag}\left(\sqrt{m_{\rm lightest}}, \sqrt{m_2^{\rm NH}}, \sqrt{m_3^{\rm NH}}\right)$, and $\sqrt{D_{\rm IH}} = {\rm diag}\left(\sqrt{m_1^{\rm IH}}, \sqrt{m_2^{\rm IH}}, \sqrt{m_{\rm lightest}}\right)$ in the minimal $B-L$ model. For the minimal seesaw in the alternative $B-L$ model, only two RHNs are involved in the seesaw mechanism and $m_{\rm lightest} = 0$. In this case, $\sqrt{D_{\rm NH/IH}}$ is expressed as 3×2 matrices as follows:

$$\sqrt{D_{\rm NH}} = \begin{pmatrix} 0 & 0 \\ \sqrt{m_2^{\rm NH}} & 0 \\ 0 & \sqrt{m_3^{\rm NH}} \end{pmatrix},$$
$$\sqrt{D_{\rm IH}} = \begin{pmatrix} \sqrt{m_1^{\rm IH}} & 0 \\ 0 & \sqrt{m_2^{\rm IH}} \\ 0 & 0 \end{pmatrix}. \tag{22}$$

With the inputs of the oscillation data, the mixing matrix $\mathcal{R}$ is found to be a function $m_{\rm lightest}$, m_N and the Majorana CP-phases. We find $|\mathcal{R}_{\alpha i}|^2$ is independent of the Majorana CP-phases, so that the heavy neutrino decay processes are determined by only two free parameters: $m_{\rm lightest}$ and m_N.

Appendix E. Heavy neutrino branching ratios in the alternative $B-L$ model

In the alternative $B-L$ model, only two RHNs are involved in the seesaw mechanism and the mixing matrix $\mathcal{R}$ is given by Eq. (21) with the 3×2 matrices in Eq. (22). It is easy to find a relation between $\mathcal{R}_{\alpha i}$ ($i = 1, 2, 3$) in the minimal $B-L$ model and $\mathcal{R}_{\alpha i}$ ($i = 1, 2$) in the alternative $B-L$ model (for vanishing Majorana phases). For the NH case, the element $\mathcal{R}_{\alpha i}$ in the alternative $B-L$ model is the same as the element $\mathcal{R}_{\alpha i+1}$ in the minimal $B-L$ model. Similarly, for the IH case, the element $\mathcal{R}_{\alpha i}$ in the alternative $B-L$ model is the same as the element $\mathcal{R}_{\alpha i}$ in the

Table 4
Branching ratios of the heavy neutrinos $N^{i=1,2}$ into $e/\mu/\tau + jj$ in the alternative $B-L$ model.

	$e+jj$	$\mu+jj$	$\tau+jj$
	NH case		
$m_N = 50$ GeV			
N^1	0.194	0.213	0.213
N^2	0.0154	0.318	0.318
$m_N = 100$ GeV			
N^1	0.189	0.208	0.208
N^2	0.0143	0.296	0.296
	IH case		
$m_N = 50$ GeV			
N^1	0.412	0.104	0.104
N^2	0.203	0.224	0.224
$m_N = 100$ GeV			
N^1	0.402	0.102	0.102
N^2	0.189	0.208	0.208

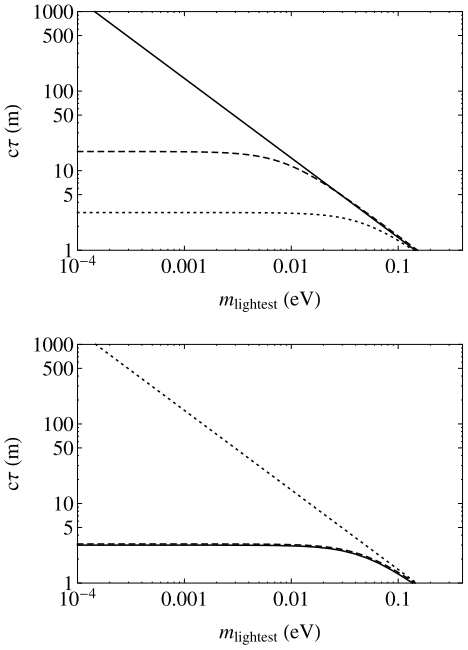

Fig. 3. Top panel: The lifetime (times speed of light) of N^1 (solid), N^2 (dashed) and N^3 (dotted) for the NH light neutrino mass spectrum, for $m_N = 50$ GeV. Bottom panel: Same as the top panel but for the IH light neutrino mass spectrum.

minimal $B-L$ model. For the alternative $B-L$ model the resultant branching ratios are listed in Table 4, corresponding to Table 3 for the minimal $B-L$ model. Because of the relation between $\mathcal{R}$ elements in the two $B-L$ models, the NH (IH) case results for $N^{1,2}$ in Table 4 for $m_N = 100$ GeV are the same as those for $N^{2,3}$ ($N^{1,2}$) in Table 3. This correspondence is not exact for the case of $m_N = 50$ GeV, since the partial decay width of Eq. (15) from the interference contributes to the total decay width. We find that this contribution is small, and the correspondence is satisfied as a good approximation. Similarly to the minimal $B-L$ model, we find the branching ratio of $N^iN^i \to \ell^\pm\ell^\pm jjjj$ for any lepton flavors to be about 20%.

Appendix F. Long-lived heavy neutrinos

In the minimal $B-L$ model, we calculate the total decay widths for $N^{1,2,3}$ as a function of m_{lightest}. We show in Fig. 3 the lifetime of $N^{1,2,3}$ for the NH (top) and IH (bottom) cases for $m_N = 50$ GeV. Fig. 4 is same as Fig. 3 but for $m_N = 100$ GeV. The longest-lived

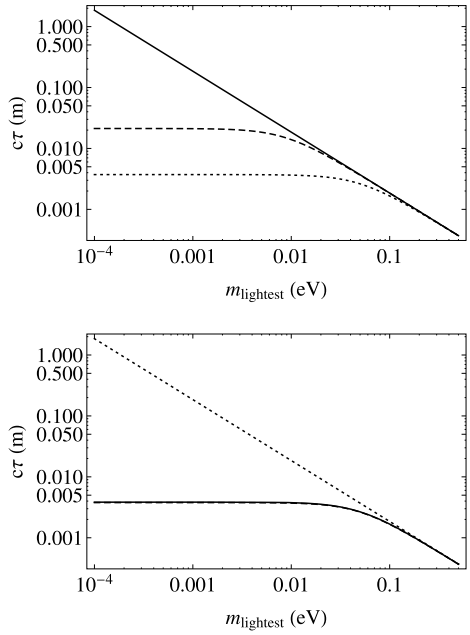

Fig. 4. Same as Fig. 3 but for $m_N = 100$ GeV.

heavy neutrino lifetime is inversely proportional to m_{lightest}, and hence it becomes a DM candidate in the limit of $m_{\text{lightest}} \to 0$.

Similarly to our discussion about the branching ratios, the lifetime of $N^{1,2}$ in the alternative $B-L$ model can be obtained from the results in Figs. 3 and 4. The lifetime of $N^{1,2}$ for the NH case is given by the lifetime of $N^{2,3}$, respectively, in the limit of $m_{\text{lightest}} \to 0$. For the IH case, the lifetime of $N^{1,2}$ corresponds to the lifetime of $N^{1,2}$, respectively, in the limit of $m_{\text{lightest}} \to 0$. However, we have to be careful. These results are true only if $v_\nu = 246$ GeV in Eq. (4). In the alternative $B-L$ model, the neutrino Dirac mass is generated from the VEV of the new Higgs doublet H_ν which only couples with neutrinos. This structure is nothing but the one in the so-called neutrinophilic two Higgs doublet model [24]. In order to avoid a significant change of the SM Yukawa couplings, we normally take $v_\nu \ll v_h \simeq 246$ GeV. This means that the actual lifetime of $N^{1,2}$ is shorten by a factor of $(v_\nu/v_h)^2 \ll 1$. However, N^1 or N^2 can still be long-lived.

References

[1] P. Minkowski, $\mu \to e\gamma$ at a rate of one out of 10^9 muon decays? Phys. Lett. B 67 (1977) 421;
T. Yanagida, Horizontal symmetry and masses of neutrinos, Prog. Theor. Phys. 64 (1980) 1103;
J. Schechter, J.W.F. Valle, Neutrino masses in SU(2) ⊗ U(1) theories, Phys. Rev. D 22 (1980) 2227;
T. Yanagida, in: O. Sawada, A. Sugamoto (Eds.), Proceedings of the Workshop on the Unified Theory and the Baryon Number in the Universe, KEK, Tsukuba, Japan, 1979, p. 95;
M. Gell-Mann, P. Ramond, R. Slansky, in: P. van Nieuwenhuizen, et al. (Eds.), Supergravity, North-Holland, Amsterdam, 1979, p. 315;
S.L. Glashow, The future of elementary particle physics, in: M. Levy, et al. (Eds.), Proceedings of the 1979 Carg'ese Summer Institute on Quarks and Leptons, Plenum Press, New York, 1980, p. 687;
R.N. Mohapatra, G. Senjanovic, Neutrino mass and spontaneous parity violation, Phys. Rev. Lett. 44 (1980) 912.
[2] R.N. Mohapatra, R.E. Marshak, Local B-L symmetry of electroweak interactions, Majorana neutrinos and neutron oscillations, Phys. Rev. Lett. 44 (1980) 1316, Erratum: Phys. Rev. Lett. 44 (1980) 1643;
R.E. Marshak, R.N. Mohapatra, Quark-lepton symmetry and B-L as the U(1) generator of the electroweak symmetry group, Phys. Lett. B 91 (1980) 222;
C. Wetterich, Neutrino masses and the scale of B-L violation, Nucl. Phys. B 187 (1981) 343;

A. Masiero, J.F. Nieves, T. Yanagida, B-L violating proton decay and late cosmological baryon production, Phys. Lett. B 116 (1982) 11;
R.N. Mohapatra, G. Senjanovic, Spontaneous breaking of global $B-L$ symmetry and matter-antimatter oscillations in grand unified theories, Phys. Rev. D 27 (1983) 254;
W. Buchmuller, C. Greub, P. Minkowski, Neutrino masses, neutral vector bosons and the scale of B-L breaking, Phys. Lett. B 267 (1991) 395.

[3] Z. Kang, P. Ko, J. Li, New avenues to heavy right-handed neutrinos with pair production at hadronic colliders, Phys. Rev. D 93 (7) (2016) 075037, arXiv:1512.08373 [hep-ph].

[4] P. Cox, C. Han, T.T. Yanagida, LHC search for right-handed neutrinos in Z' models, J. High Energy Phys. 1801 (2018) 037, arXiv:1707.04532 [hep-ph].

[5] E. Accomando, L. Delle Rose, S. Moretti, E. Olaiya, C.H. Shepherd-Themistocleous, Extra Higgs boson and Z′ as portals to signatures of heavy neutrinos at the LHC, J. High Energy Phys. 1802 (2018) 109, arXiv:1708.03650 [hep-ph].

[6] A. Das, N. Okada, D. Raut, Enhanced pair production of heavy Majorana neutrinos at the LHC, Phys. Rev. D 97 (11) (2018) 115023, arXiv:1710.03377 [hep-ph].

[7] A. Das, N. Okada, D. Raut, Heavy Majorana neutrino pair productions at the LHC in minimal U(1) extended standard model, Eur. Phys. J. C 78 (9) (2018) 696, arXiv:1711.09896 [hep-ph].

[8] S. Jana, N. Okada, D. Raut, Displaced vertex signature of type-I seesaw model, Phys. Rev. D 98 (3) (2018) 035023, arXiv:1804.06828 [hep-ph].

[9] K. Fujii, et al., arXiv:1710.07621 [hep-ex].

[10] J.C. Montero, V. Pleitez, Gauging U(1) symmetries and the number of right-handed neutrinos, Phys. Lett. B 675 (2009) 64, arXiv:0706.0473 [hep-ph].

[11] M. Carena, A. Daleo, B.A. Dobrescu, T.M.P. Tait, Z' gauge bosons at the Tevatron, Phys. Rev. D 70 (2004) 093009, arXiv:hep-ph/0408098;
J. Heeck, Unbroken B-L symmetry, Phys. Lett. B 739 (2014) 256, arXiv:1408.6845 [hep-ph].

[12] S.F. King, Large mixing angle MSW and atmospheric neutrinos from single right-handed neutrino dominance and U(1) family symmetry, Nucl. Phys. B 576 (2000) 85, arXiv:hep-ph/9912492;
P.H. Frampton, S.L. Glashow, T. Yanagida, Cosmological sign of neutrino CP violation, Phys. Lett. B 548 (2002) 119, arXiv:hep-ph/0208157.

[13] N. Okada, S. Okada, D. Raut, A natural Z'-portal Majorana dark matter in alternative U(1) extended standard model, arXiv:1811.11927 [hep-ph].

[14] M. Aaboud, et al., ATLAS Collaboration, Search for new high-mass phenomena in the dilepton final state using 36 fb^{-1} of proton-proton collision data at $\sqrt{s}=$ 13 TeV with the ATLAS detector, J. High Energy Phys. 1710 (2017) 182, arXiv:1707.02424 [hep-ex].

[15] A.M. Sirunyan, et al., CMS Collaboration, Search for high-mass resonances in dilepton final states in proton-proton collisions at $\sqrt{s}=$ 13 TeV, J. High Energy Phys. 1806 (2018) 120, arXiv:1803.06292 [hep-ex].

[16] J. Pumplin, D.R. Stump, J. Huston, H.L. Lai, P.M. Nadolsky, W.K. Tung, New generation of parton distributions with uncertainties from global QCD analysis, J. High Energy Phys. 0207 (2002) 012, arXiv:hep-ph/0201195.

[17] N. Okada, S. Okada, Z'_{BL} portal dark matter and LHC Run-2 results, Phys. Rev. D 93 (7) (2016) 075003, arXiv:1601.07526 [hep-ph];
N. Okada, S. Okada, Z'-portal right-handed neutrino dark matter in the minimal U(1)$_X$ extended Standard Model, Phys. Rev. D 95 (3) (2017) 035025, arXiv:1611.02672 [hep-ph].

[18] For a review, see S. Okada, Z' portal dark matter in the minimal $B-L$ model, Adv. High Energy Phys. 2018 (2018) 5340935, arXiv:1803.06793 [hep-ph].

[19] https://cds.cern.ch/record/2285582?ln=en.

[20] A. Anisimov, P. Di Bari, Cold dark matter from heavy right-handed neutrino mixing, Phys. Rev. D 80 (2009) 073017, arXiv:0812.5085 [hep-ph];
N. Okada, O. Seto, Higgs portal dark matter in the minimal gauged $U(1)_{B-L}$ model, Phys. Rev. D 82 (2010) 023507, arXiv:1002.2525 [hep-ph].

[21] C. Patrignani, et al., Particle Data Group, Review of particle physics, Chin. Phys. C 40 (10) (2016) 100001.

[22] K. Abe, et al., T2K Collaboration, Combined analysis of neutrino and antineutrino oscillations at T2K, Phys. Rev. Lett. 118 (15) (2017) 151801, arXiv:1701.00432 [hep-ex].

[23] P. Adamson, et al., NOvA Collaboration, First measurement of electron neutrino appearance in NOvA, Phys. Rev. Lett. 116 (15) (2016) 151806, arXiv:1601.05022 [hep-ex].

[24] E. Ma, Naturally small seesaw neutrino mass with no new physics beyond the TeV scale, Phys. Rev. Lett. 86 (2001) 2502, arXiv:hep-ph/0011121;
F. Wang, W. Wang, J.M. Yang, Split two-Higgs-doublet model and neutrino condensation, Europhys. Lett. 76 (2006) 388, arXiv:hep-ph/0601018;
S. Gabriel, S. Nandi, A new two Higgs doublet model, Phys. Lett. B 655 (2007) 141, arXiv:hep-ph/0610253;
S.M. Davidson, H.E. Logan, Dirac neutrinos from a second Higgs doublet, Phys. Rev. D 80 (2009) 095008, arXiv:0906.3335 [hep-ph];
N. Haba, M. Hirotsu, TeV-scale seesaw from a multi-Higgs model, Eur. Phys. J. C 69 (2010) 481, arXiv:1005.1372 [hep-ph].